Sensitive high-resolution white-light Schlieren technique with a large dynamic range for the investigation of ablation dynamics

Alfred Vogel, Ingo Apitz, and Sebastian Freidank

Institute of Biomedical Optics, University of Lübeck, Peter-Monnik Weg 4, D-23562 Lübeck, Germany

Rory Dijkink

Physics of Fluids Group, Faculty of Science and Technology, University of Twente, P.O. Box 217, 7500 AE Enschede, The Netherlands

Received January 27, 2006; revised March 22, 2006; accepted March 24, 2006; posted April 5, 2006 (Doc. ID 67571)

We developed a modified Hoffman contrast technique with a 12 ns pulsed incoherent extended white-light source that enables an easily interpretable visualization of ablation plumes with high resolution, a large dynamic range, and color information. By comparison, a conventional dark-field setup with a slitlike laser light source provides large sensitivity but a small dynamic range, and it is difficult to interpret the filtered images. © 2006 Optical Society of America

OCIS codes: 120.4820, 170.1020, 350.3390.

Knowledge about plume dynamics in pulsed laser ablation is important for thin-film deposition, the creation of debris-free structures in materials processing, and the control of shielding effects. Moreover, analysis of the plume dynamics and of the stress distribution below the target surface helps to clarify the kinetics of phase transitions underlying ablation.

Visualization of phase objects in ablation plumes is challenging because the refractive-index variations are usually smaller in gases than in liquids or solids, and the small size of the plumes results in short interaction lengths with the illuminating light producing only small deflections.[1] When ablation is performed in a background gas, the plume dynamics is intricate, involving the generation of an external and an internal shock wave followed by the evolution of a mushroomlike cloud.[2,3] The internal shock wave propagates back toward the target, interacts with the ongoing flow of ablated material, and thus influences the entire plume dynamics. This interaction has to date been studied only by use of numerical and analytical models that assume a spherical symmetry.[4,5] Experimental analysis of the actual complexity requires improved Schlieren techniques.

In this Letter, we introduce a modified Hoffman modulation contrast technique exhibiting an approximately sevenfold increased sensitivity without a loss of dynamic range. The original Hoffman technique was developed for microscopic inspection of biological phase objects[1,6] and has not yet been employed for the visualization of phase structures in ablation plumes. We demonstrate the performance of the modified Hoffman technique on pulsed laser ablation of water and compare it with more conventional Schlieren techniques.[1]

Figure 1 shows the setup with the shapes of light sources and Schlieren filters investigated. The filters are located in the back focal plane (Fourier plane) of the first imaging lens, L_1. Phase information in the object plane is transformed into intensity information in the image plane by blocking parts of the spatial frequency spectrum.[1,7] In each Schlieren technique, the shape of the light source in the plane conjugate to the Fourier plane must match the shape of the filter.

For the bright-field, knife-edge, and Hoffman contrast images we used a plasma discharge lamp with 12 ns duration (Nanolite), and for the dark-field images we employed 6 ns frequency-doubled Nd:YAG laser pulses that were coupled into a 300 m long multimode optical fiber to destroy temporal coherence. The fiber tip, with a 160 μm core diameter and a numerical aperture NA=0.22, served as the light source for speckle-free photography. After passage through the fiber, the pulse duration was prolonged to 18 ns (FWHM). This exposure time yields sharp images of structures 2–100 μm in size moving with a velocity of up to 110–5550 m/s, respectively. Test objects were created by water ablation using 80 ns Er:YAG laser pulses and 150 ns thulium laser pulses and by skin ablation with 200 μs Er:YAG laser pulses.

Images taken with the different modalities are presented in Fig. 2. Contrast in the bright-field image in

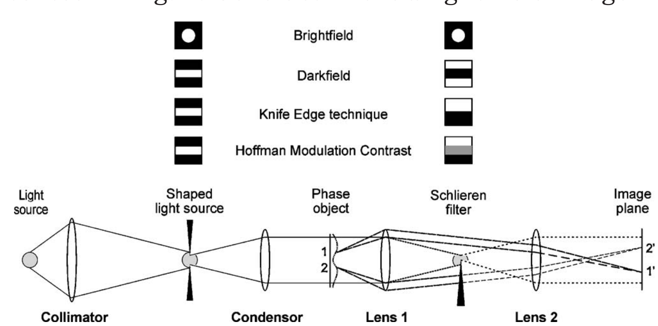

Fig. 1. Schlieren setup with matched pairs of shapes of light sources and filters. Lenses used: Nikon 50 mm/1.2 for collimation, Pentax 50 mm/1.7 as condensor, Nikon 105 mm/2.8 as L_1, Achromat f=400 mm as L_2.

0146-9592/06/121812-3/$15.00

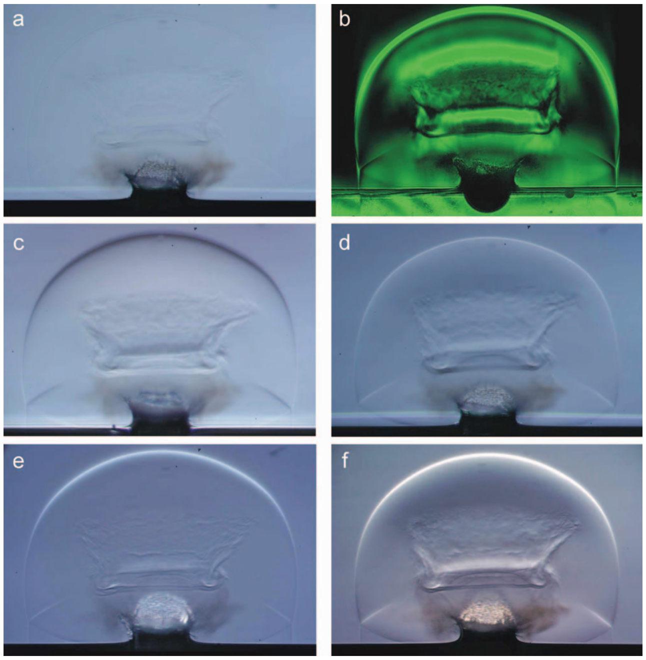

Fig. 2. Ablation plume produced during water ablation with 80 ns Er:YAG laser pulses ($\lambda=2.94\ \mu m$, $\Phi=5.4\ J/cm^2$, spot diameter 0.5 mm). a, Bright-field image recorded with $F=11$. b, Dark-field image obtained with a 100 μm filter wire. c, Knife-edge technique, with the lower part of the Fourier plane blocked. d, Knife-edge technique, with filter from above. e, Hoffmann modulation contrast. f, Combined Hoffmann modulation and knife-edge technique, with 1/7 of the image of the light source uncovered. All images were taken 2.3 μs after the laser pulse and have a size of 5.5 mm $\times$ 3.8 mm in object space.

Fig. 2(a) arises from phase gradients that deflect light out of the imaging aperture. The sensitivity is poor because contrast is produced only if the deflection angle exceeds a certain NA-dependent threshold. Sensitivity may be increased by reducing the NA, but that results in a low diffraction-limited resolution.

A much higher sensitivity without resolution loss is achieved when all nondeflected light is blocked by the filter and only deflected light reaches the image plane (dark-field technique). The sensitivity now relies on the ratio of the size of the spatial frequency spectrum to the size of the blocking filter; i.e., it is proportional to the focal length of L_1 and inversely proportional to the filter size. High sensitivity thus requires a small light source. We used a lens with 200 mm focal length and a horizontally oriented 100 μm thin filtering wire. This filter enabled us to use a slitlike light source that makes better use of the available light than is possible with a dotlike Schlieren filter, which requires a point source. Nevertheless, only the laser source but not the plasma spark had sufficient brightness to produce dark-field images with this setup. Results are shown in Figs. 2(b) and 3. The sensitivity is excellent: in Fig. 3 even weak acoustic transients arising from the individual spikes in free-running laser irradiation are well visible. Disadvantages are coherent artifacts[1] and the fact that refractive-index gradients with opposite sign look alike in the filtered image. Therefore, the leading and trailing edges of a shock wave appear as bright lines separated by a black line originating from the pressure peak where no light is deflected. Thus, one can easily misinterpret leading and trailing edge as separate entities instead as parts of one physical structure.

By contrast, the knife-edge technique produces information on the sign of the phase gradients [Figs. 2(c) and 2(d)]. The background of the filtered image is gray because part of the image of the light source is covered by the knife edge. Deflection in the upward direction produces brightening, because more light passes the filter ($1\rightarrow1'$ in Fig. 1), and deflection in the opposite direction results in darkening ($2\rightarrow2'$). Phase objects thus have a relieflike, easily interpretable appearance. The brightness change is proportional to the angle of deflection and inversely proportional to the width of the illumination slit. An extended light source thus yields a large dynamic range, and a small slit results in high sensitivity, but the saturation values of maximum brightness and darkness are soon reached. Usually, the knife edge blocks more than 50% of the nondeflected light because brightness variations in the detected image are perceived with optimum contrast when the knife edge covers about 85% of the image of the light source. This is due to the logarithmic sensitivity characteristics of the human eye. Moreover, a large cutoff increases the sensitivity of the knife-edge technique.[1] Unfortunately, these advantages are compromised by the fact that a large part of the spatial frequency spectrum of the phase object is blocked, which considerably deteriorates resolution.

This problem is overcome by the Hoffman modulation contrast method.[6] Here a narrow gray filter absorbing 85% of the incident light is attached to the opaque knife edge and matched with the image of the light source (Fig. 1). The 15% light transmitted through the gray filter not only creates the necessary background intensity for the visualization of phase gradients but also carries information about the phase object. Thus, a larger part of the spatial frequency spectrum contributes to image formation than with the knife-edge technique, and the resolution is much better, as is visible by comparison of Figs. 2(d) and 2(e).

The image in Fig. 2(e) was taken with a commercially available modulation contrast filter for micros-

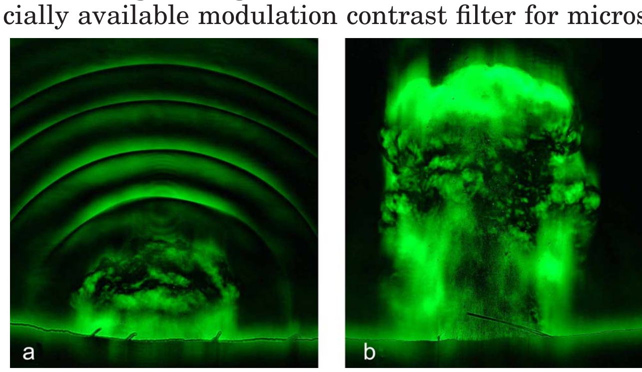

Fig. 3. (Color online) Dark-field images of the acoustic transients and ablation plume during skin ablation with a 200 μs Er:YAG laser pulse ($\lambda=2.94\ \mu m$, $\Phi=20\ J/cm^2$, spot size 2.3 mm), a, 22.5 μs and b, 40 μs after the onset of the pulse. Image size: 7.5 mm $\times$ 10.0 mm.

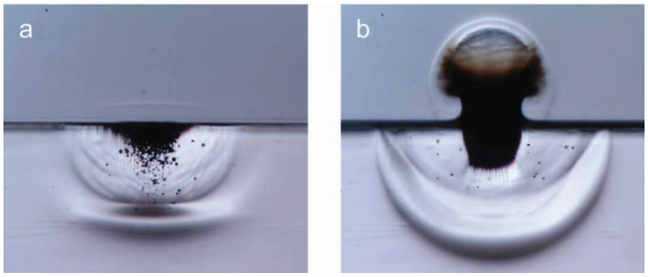

Fig. 4. Water ablation with a 150 ns, 120 mJ thulium laser ($\lambda = 2.0\ \mu m$), photographed 800 ns after the laser pulse by use of the modified Hoffman technique. The radiant exposure and spot size were 6 J/cm^2 and 850 μm in a and 60 J/cm^2 and 300 μm in b. Image size: 3.5 mm $\times$ 3.5 mm.

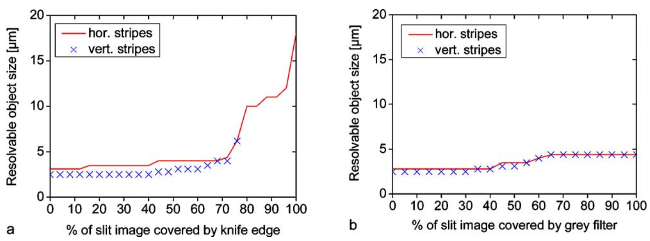

Fig. 5. (Color online) Relation between optical resolution and percent cutoff for, a, the knife-edge technique and, b, modified Hoffman modulation contrast. The resolution was determined by using a U.S. Air Force test plate. In a no vertical stripes could be resolved for more than 75% cutoff.

copy (Leica Microsystems) with a 1.38 mm wide gray stripe. The characteristic width of this Schlieren filter is 27.6 times larger than the thickness of the wire used for producing the dark-field image of Fig. 2(b). Correspondingly, the dynamic range is large enough to avoid saturation effects even in the image of the shock wave running ahead of the plume. However, finer structures within the plume are displayed with little contrast. To increase sensitivity without sacrificing dynamic range or resolution, we introduced a modification of the Hoffman technique. Now, the gray part covers only 87% of the image of the light source, leaving 13% free, and the border of the gray part acts as a knife edge. With this combination of Hoffman modulation contrast and knife-edge technique, the fractions of light transmitted through the gray filter and passing it contribute exactly equally to the background intensity in the filtered image (15% transmission through the gray filter covering 87% of the relevant area corresponds to 13% of the incident light, the same percentage as transmitted through the uncovered region). The knife-edge part of the combined technique is very sensitive because the uncovered part of the light source image is narrow. Small deflections shifting the image of the light source by only $\approx 1/7$ part of the width of the gray filter suffice to double the intensity in the filtered image or to reduce it by 50%. Light modulation by the gray filter, in turn, provides a 7 times larger dynamic range than the knife-edge part of the filtering. The dependence between light deflection and intensity change in the filtered image in Fig. 2(f) is nonlinear, stronger for small deflections and weaker for large deflections. The resolution is not compromised because the transmitted part of the spatial frequency spectrum is even larger than with the regular Hoffman technique.

The image in Fig. 2(f) obtained with the new technique yields more detailed information on the ablation plume than could previously be visualized. The upper part of the plume consists of water vapor resulting from complete vaporization of the top target layer, and the lower part consists of a mixture of vapor and droplets resulting from a phase explosion.[3] The reddish color of the droplets is indicative of Rayleigh scattering and thus reveals their very small size.[3] The plume expansion has produced an external shock wave that is partly reflected at the water surface, where the nonlinear interaction of incident and reflected waves results in a Mach stem. Moreover, the collision between plume and ambient air has produced an internal shock wave that travels back through the central part of the plume, generating a ring vortex in the plume periphery.

Figure 4 illustrates that the new technique is also well suited for the visualization of subsurface stress waves. With increasing radiant exposure, the stress wave evolves from a bipolar thermoelastic wave into a monopolar wave driven by a phase explosion.

The resolution of the modified Hoffman method in comparison with the knife-edge technique, measured by using a U.S. Air Force test plate, is shown in Fig. 5. Resolution is dramatically improved in the regime with largest sensitivity, in which a large part of the light source is covered by the knife edge or the gray part of the filter.

Other microscopic Schlieren techniques are less suited for the investigation of ablation dynamics. Phase contrast is very sensitive for the visualization of thin phase objects introducing phase shifts $\Delta\rho$,[7] but phase gradients such as those commonly found in ablation plumes lead to light deflection off the phase ring, resulting in disturbing halos.[1,6] The performance of differential interference contrast is similar to that of the normal Hoffman technique,[1,6] but the complex optical setup cannot easily be established with the large working distances necessary for the imaging of ablation plumes.

This work was supported by the U.S. Air Force Office of Scientific Research under grant FA8655-02-1-3047. A. Vogel's e-mail address is vogel@bmo.uni-luebeck.de.

References

1. G. S. Settles, *Schlieren and Shadowgraph Techniques* (Springer, 2001).
2. A. Vogel and V. Venugopalan, Chem. Rev. **103**, 577 (2003).
3. I. Apitz and A. Vogel, Appl. Phys. A **81**, 329 (2005).
4. H. L. Brode, Phys. Fluids **2**, 217 (1959).
5. N. Arnold, J. Gruber, and J. Heitz, Appl. Phys. A **69**, S93 (1999).
6. R. Hoffman and L. Gross, Appl. Opt. **14**, 1169 (1975).
7. W. Lauterborn and T. Kurz, *Coherent Optics* (Springer, 2003).